BIOCHEMISTRY
including biophysical chemistry & molecular biology

Article

pubs.acs.org/biochemistry

Photocycle and Vectorial Proton Transfer in a Rhodopsin from the Eukaryote *Oxyrrhis marina*

Christian Janke,[†] Frank Scholz,[‡] Johanna Becker-Baldus,[§] Clemens Glaubitz,[§] Phillip G. Wood,[†] Ernst Bamberg,[†] Josef Wachtveitl,[‡] and Christian Bamann*[,†]

[†]Max-Planck-Institut für Biophysik, Max-von-Laue Strasse 3, 60438 Frankfurt am Main, Germany

[‡]Institute of Physical and Theoretical Chemistry and [§]Institute for Biophysical Chemistry & Centre for Biomolecular Magnetic Resonance, Johann Wolfgang Goethe-Universität, Max-von-Laue Strasse 7, 60438 Frankfurt am Main, Germany

Supporting Information

ABSTRACT: Retinylidene photoreceptors are ubiquitously present in marine protists as first documented by the identification of green proteorhodopsin (GPR). We present a detailed investigation of a rhodopsin from the protist *Oxyrrhis marina* (OR1) with respect to its spectroscopic properties and to its vectorial proton transport. Despite its homology to GPR, OR1's features differ markedly in its pH dependence. Protonation of the proton acceptor starts at pH below 4 and is sensitive to the ionic conditions. The mutation of a conserved histidine H62 did not influence the pK_a value in a similar manner as in other proteorhodopsins where the charged histidine interacts with the proton acceptor forming the so-called His-Asp cluster. Mutational and pH-induced effects were further reflected in the temporal behavior upon light excitation ranging from femtoseconds to seconds. The primary photodynamics exhibits a high sensitivity to the environment of the proton acceptor D100 that are correlated to the different initial states. The mutation of the H62 does not affect photoisomerization at neutral pH. This is in agreement with NMR data indicating the absence of the His-Asp cluster. The subsequent steps in the photocycle revealed protonation reactions at the Schiff base coupled to proton pumping even at low pH. The main electrogenic steps are associated with the reprotonation of the Schiff base and internal proton donor. Hence, OR1 shows a different theme of the His-Asp organization where the low pK_a of the proton acceptor is not dominated by this interaction, but by other electrostatic factors.

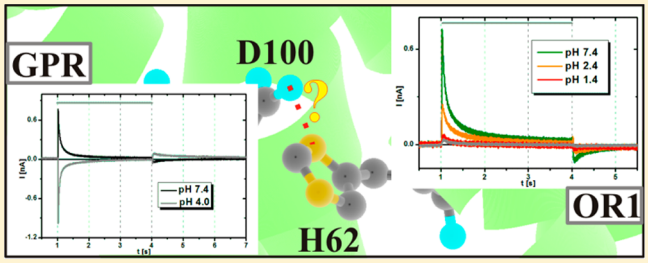

The heterotrophic dinoflagellate *Oxyrrhis marina* represents an important model organism for marine ecology.[1] The morphospecies *Oxyrrhis marina* derived from an early branch point in the evolution of dinoflagellates. Therefore it possesses cytological features which are distinct from the phylum dinophyceae such as nuclear division.[2] Its phylogenetic position renders *Oxyrrhis marina* a model organism for the evolution of genes and organelles.[3] Two recent publications revealed the existence of a strongly expressed rhodopsin in *Oxyrrhis marina* (named OR1). It belongs to the proteorhodopsin (pR) family[4,5] and has been presumably acquired from lateral gene transfer similar to other pR-like molecules.[6] Different conclusions were drawn about its biological function from phototactic and cell localization experiments. A photosensoric function of a rhodopsin was found in phototactic experiments corroborated by the response sensitivity toward hydroxylamine that bleaches retinal containing photoreceptors.[5] On the contrary, Slamovits et al. found an endomembrane localization of a strongly expressed rhodopsin that they attributed to a phototrophic function.[4]

In eukaryotes, several type I rhodopsins have been identified and characterized before that are not members of the pR family, in particular from algae[7,8] or from fungi.[9] In several cases, their involvement in phototaxis is well documented,[10] while in others their native function is elusive. In host systems, they can work as a proton pump leading to speculation about their contribution to light energy conversion (e.g., ref 11). In fact, the awareness of retinal-based photosynthesis started with the discovery of bacteriorhodopsin (bR).[12] After the identification of a eubacterial green proteorhodopsin (GPR),[13] retinal dependent light energy fixation turned into a global phenomenon by the ubiquitous presence of pR-like genes in all kingdoms.[14] All pRs described so far share the general features of type I rhodopsins with the seven transmembrane helices and a retinal chromophore linked to a lysine side chain via a protonated Schiff base (pSB).[15−17] As in the proton pump bR, absorption of a photon initiates a photocycle in GPR consisting of a series of spectrally distinct intermediates (K, L, M, N, O).[17,18] The primary process in this photocycle is an isomerization of the retinal chromophore from its *all-trans* state to 13-*cis* leading to the formation of the first ground state photoproduct (termed K-intermediate in bR).[19] Subsequently,

Received: October 17, 2012
Revised: March 26, 2013
Published: March 27, 2013

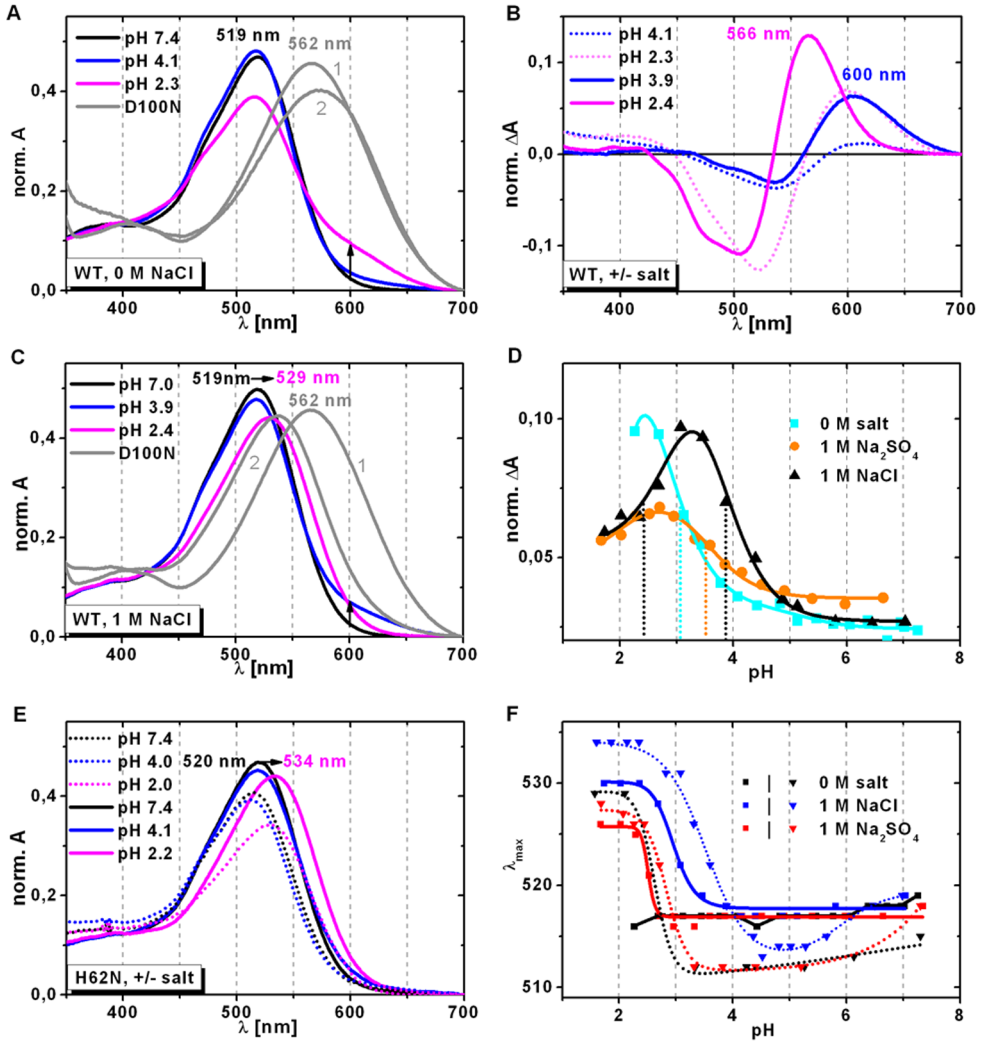

Figure 1. pH-titration of OR1. (A) Absorbance spectra of OR1 wild type under salt-free conditions and the D100N mutant (gray lines) at pH 7.2 (1) and pH 2.3 (2). Wild type spectra are normalized to A_{280nm}, and the D100N is scaled to the maximum at 519 of the wild type at pH 7.4. (B) Difference spectra of OR1 at acidic pH values under salt-free conditions (dotted lines) and with 1 M NaCl (line). The wild type spectrum at pH 7.2 was taken as reference (S_{ref}). (C) Absorbance spectra of OR1 wild type and the D100N mutant at 1 M NaCl (gray lines) at pH 7.4 (1) and pH 2.3 (2). All spectra were as well normalized to $A_{280\ nm}$. D100N is scaled to the maximum at 519 of the wild type at pH 7.0 (D) Transition from S_{ref} to S_{600nm} followed by the absorbance changes at 600 nm. The dotted lines indicate the half-maximal amplitude change and are color coded according to the ionic conditions in the legend. The absorbance changes are normalized to the protein concentration at 280 nm. (E) Absorbance spectra of OR1 H62N at different pH values under salt-free conditions (dotted lines) and with 1 M NaCl (lines). (F) The pH dependence of the λ_{max} values for the wild type (squares) and the H62N (triangles) mutant under different ionic conditions.

the Schiff base deprotonates and the released proton moves toward the extracellular side with D97 (D85 in bR) as the primary proton acceptor. Reprotonation of the Schiff base from E108 (D96 in bR) located at the cytoplasmic side establishes the vectorial proton transport.

The primary proton acceptor D97 in GPR has an unusual high pK_a of 7.7 that is provoked by the conserved H75 residue forming a pH-dependent hydrogen-bonded proton dyad with D97 as it has been shown by solid-state NMR measurements.[20] The close proximity of these two residues has also been described in the solution NMR structure of GPR[21] and the X-ray structure of xanthorhodopsin (XR).[16] The protonation state of D97 in GPR defines the vectoriality of the proton transport.[22] At high pH with a deprotonated D97, an outward transport occurs as in bR although the sequence of the individual proton transfer steps differs. This is mainly due to a different proton release complex toward the extracellular side that leads to a retarded proton release in the photocycle.[17] The outward proton transport declines as the proton acceptor D97 is protonated at low pH,[23] where an inward transport has been described in a two photon photocycle.[22] However, GPR is able to create a proton gradient that is high enough to be utilized for ATP synthesis *in vivo*.[24,25] As pRs appear ubiquitous in marine microorganisms, their ecological role has been estimated to have a high impact, either for primary energy fixation or as a power supply to drive different cellular processes in the way that has been discussed in the case of OR1.[14]

The general role of the conserved histidine in the pR family has been challenged by the recently described rhodopsin from *Exiguobacterium sibiricum* (ESR).[26] Here, the histidine stabilizes the deprotonated proton acceptor D85 in the initial state and during the photocycle in such pH-dependent manner that proton pumping is retained even at low pH. The titration of D85 shows complex features indicating coupling to at least one

dx.doi.org/10.1021/bi301412n | *Biochemistry* 2013, 52, 2750−2763

other group. Only at high pH, when the histidine is presumably in its uncharged state, or in histidine deficient mutants, the deprotonated M-state accumulates in ESR and its amount correlates with the pH-titration curve of the proton acceptor.

Our studies were motivated by the question of the proton pumping ability of the eukaryotic pR OR1 and its relation to the photocycle and by exploring a putative role of the conserved histidine H62. We address these topics by a combination of spectroscopic and electrophysiological techniques. First we describe the expression and initial state properties of OR1. Solid-state NMR data specifically allows the determination of the uncharged state of H62 at neutral pH. The pH-titration data that give information about the charge state of the counterion at the pSB revealed a high complexity and sensitivity toward the ionic conditions: Two transitions are observed upon lowering the pH below 4 that we interpret as the protonation of the proton acceptor D100 coupled to at least one further group. In the first transition, only a fraction of the molecules are protonated resembling in their spectral properties the D100N mutant at neutral pH. The second protonation event requires high ionic strength to be observable in the wild type and the D100N mutant. This requirement is abolished by the replacement of H62 while keeping the transition's low pK_a. However, the first transition is not observable any more in the H62N mutant. In a second step, we probe the photoisomerization kinetics in different initial states in ultrafast pump−probe experiments that are very sensitive to the electronic and hydrogen-bonding environment of the pSB. The results are discussed in comparison to the D100N as a reference of a protonated counterion and to the H62N mutant that shows no difference to the wild type at neutral pH in line with the absence of the His-Asp cluster. In the third part, we turn to later steps of the photocycle and its relation to the proton pumping. In accordance with the titration data and the results from the pump−probe measurements, the deprotonated state of the Schiff base (M-state) can be followed at low pH and current measurements of reconstituted OR1 can be correlated to proton pumping even at pH 2.4. The H62N mutation had no strong impact on the general appearance of the deprotonated state, but modulated its accumulation during the photocycle. A part of this effect seems to be independent of the charge of the histidine and could be rather related to its influence on other groups than D100. Therefore, we find another variation of the His-Asp theme in OR1.

EXPERIMENTAL PROCEDURES

Cloning and Expression. The nucleotide sequence of OR1 (Acc. No. ABV22426) was optimized to human codon usage and synthesized (Sloning Biotechnology GmbH, Puchheim, Germany). The *or1* gene was cloned into the *Bam*HI/*Hin*dIII site of the vector pCDNA 3.1 (−) containing a C-terminal *eyfp* gene for expression in NG108−15 cells. The cells were transfected with cDNA using either Effectene (Qiagen) or Lipofectamine 2000 (Invitrogen). For protein purification the gene was cloned into the *Eco*RI/*Not*I site of the vector pPiK9K (Invitrogen). Point mutations were generated by PCR site-directed mutagenesis. The *Pichia pastoris* strain *SMD1163* (*his4*, *pep4*, *prB1*) (Invitrogen) was transformed with 3 μg of linearized vector (pPik9K::opsin_or1). Selection on geniticin and cell culture was followed by the manufacturer's instructions. The expression of OR1 was induced with 1% methanol and 1 μM *all-trans* retinal during the late logarithmic phase. After cell lysis with glass beads (0.25 mm in diameter), the total membrane fraction was prepared by differential centrifugation (1 h, 100000*g*) and the membranes were solubilized in 1% dodecylmaltoside (DDM, Glycon Biochemicals) in 20 mM Hepes, 1 M NaCl, pH 7.4. The protein was purified on a Ni-NTA column. We used ClustalX 2.0 for sequence alignments.[27] Retinal extraction was carried out as described earlier.[28] ^{15}N-labeling was performed in buffered minimal methanol medium (BMM, Invitrogen) containing 5 g/L ^{15}N-ammonium chloride. For black lipid membrane experiments OR1 was reconstituted into proteoliposomes with a protein:lipid ratio of 1:5 (w/w) consisting of dioleoylphosphatidylcholine. For NMR experiments the protein:lipid ratio was increased to 1:1 (w/w).

Solid-State NMR. Magic angle spinning (MAS)-NMR experiments were carried out on a Bruker Avance III 850 MHz solid-state NMR spectrometer using a triple resonance 4 mm DVT probehead. ^{15}N cross-polarization experiments were performed using standard settings. A sample spin rate of 12 kHz was used with the sample temperature set to 270 K resulting in a real temperature inside of the MAS rotor of approximately 280 K. A recycle delay of 3 s, a contact time of 2 ms and proton decoupling of 85 kHz during a 20 ms acquisition period were applied. The spectrum shown in Figure 2 was recorded using 8k scans. ^{15}N chemical shift referencing

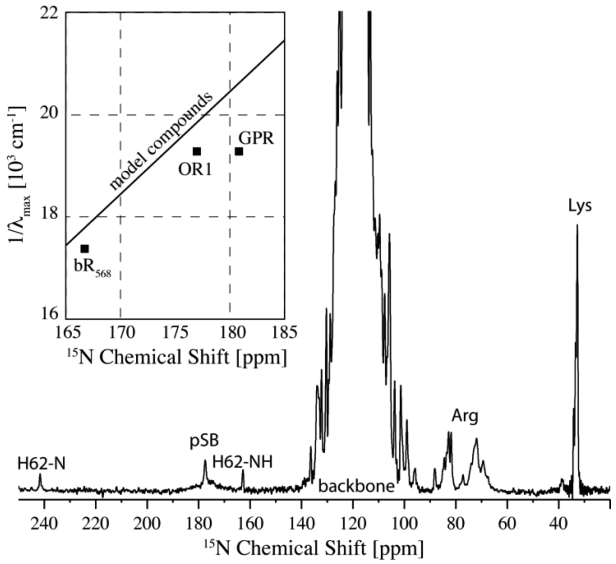

Figure 2. ^{15}N-CP-MAS NMR spectrum of U-^{15}N-OR1 at pH 7.4 reconstituted in DOPC. The signal of the protonated Schiff base (pSB) is observed at 177.5 ppm. The ^{15}N imidazole ring resonances of highly conserved H62 are detected at 162.8 ppm and 241.6 ppm. The inset shows the correlation between λ_{max} and ^{15}N chemical shifts of the pSB obtained from retinal derivatives with *all-trans* polyene chains with different halide counterions.[65] OR1 as well as *all-trans* bR (BR568) deviate not as much from model behavior as GPR.[66].

was done via the gyromagnetic ratios through the ^{13}C chemical shift of admantane with respect to DSS (4,4-dimethyl-4-silapentane-1-sulfonic acid).

Spectroscopy and Data Analysis. Static spectra were taken with a U3000 double-beam spectrophotometer (Hitachi, Japan). Titration experiments were done in a buffer containing 10 mM citrate, 10 mM Mes, 10 mM Hepes and 10 mM Tris with varying concentration of NaCl. Small volumes of acid and base were used to adjust the pH between recordings of the spectra. Light-induced absorption changes were recorded with a

dx.doi.org/10.1021/bi301412n | *Biochemistry* 2013, 52, 2750−2763

home-built flash photolysis setup. The time resolution was limited to 5 μs. Thermostated samples of OR1 ($A_{520nm} \sim 0.4$) were excited with a 10 ns laser flash from an excimer laser pumped dye laser (Coumarin 307, 503 nm, 2.5 mJ). Light from a 75 W XBO lamp was filtered by a set of 14 small-bandwidth interference filters (from 381 to 680 nm; Schott, Mainz, Germany) and passed through the sample and a monochromator (minichrom, Optometrics), before it was detected on a photodiode (UV-005, OSI Optoelectronics). The signal was amplified (PMT-4, Scientific Instruments, Gilching, Germany) and recorded on two digital storage oscilloscopes (Pro10 and Sigma30, Nicolet, USA). To improve the signal-to-noise ratio, we averaged 32 traces for each wavelength. The data sets were interpolated logarithmically. A global fitting routine was used to determine the relaxation time constants (Origin 7.5, OriginLab) and analyzed in the framework of a linear model of the photocycle as described earlier:[29]

$$\Delta A(\lambda, t) = \sum_{i=1}^{n} A_i \cdot e^{k_i t}$$

$$P_0 \xrightarrow{h\nu} P_1 \xrightarrow{k_1} P_2 \ldots P_n \xrightarrow{k_n} P_0$$

where the time-dependent absorbance changes Abs(λ,t) are analyzed by a sum of exponential functions. The rate constants k_i from the global fit describe the irreversible transitions between the kinetic intermediates P_i in decreasing order while the amplitudes A_i are identified as the decay-associated spectra (DAS) between the transitions.

The conditions for the pump−probe measurements were 1 M NaCl, 0.01% DDM and either 20 mM Hepes (pH 7.4) or 20 mM Citrate (pH 2.5) or 20 mM carbonate (pH 9). The details of the employed femtosecond spectrometer were described earlier.[19,30] For the time-resolved absorption spectroscopy a Clark CPA 2001 as source for femtosecond laser pulses with a central wavelength of 775 nm was used. The laser operates at a repetition rate of 1 kHz. The wavelength of the pump pulse was chosen at the particular pH-dependent absorption maximum of the chromophore (λ = 527 nm for pH 2.5 and λ = 522 nm for pH 9) using a home-built noncollinear optical parametric amplifier (NOPA).[31] The pump pulses were adjusted to a low energy (20 nJ/pulse) to avoid multiexcitation. The absorption changes were measured by probe pulses consisting of a single-filament white-light continuum. These pulses were generated by focusing the laser fundamental into a sapphire crystal. The probe pulses were divided into a signal and a reference part for a higher signal-to-noise ratio and recorded by two 42-segment diode arrays. The temporal resolution of the setup was about 40 to 90 fs depending on the probe wavelength.

Electrophysiological Experiments. Electrometric measurements were performed as described before[32] in 20 mM HEPES, 100 mM NaCl, pH 7.4. The proteoliposomes were adsorbed to the "trans" side of the black lipid membrane (BLM) leading to a capacitive coupling. Voltage changes across the compound membrane were recorded after excitation of OR1 with a 503 nm laser flash of 10 ns from an excimer laser pumped dye laser (Coumarin 307). The time resolution is limited by the electronics ($\tau_{10-90\%} \sim 2$ μs). The stationary proton transport currents were recorded after addition of the ionophores carbonyl cyanide *m*-chlorophenylhydrazone (CCCP) at a concentration of 6 μM or 1799/monensin (1 μM/10 μM). The membrane was illuminated with filtered light from a 75 W XBO. The action spectrum and the pH titration were done on a solid-supported membrane (SSM) system[33] (SURFE^{2}R One instrument; Scientific Devices, Heidelberg, Germany). Whole-cell patch-clamp experiments were done under voltage-clamp conditions (HEKA EPC 10 system). Glass capillaries were made from borosilicate glass capillaries with a resistance between 4 and 5 MΩ (Science Products). The bath solution consisted of 140 mM NaCl, 2 mM $CaCl_2$, 2 mM $MgCl_2$ and 10 mM Hepes (pH 7.4, NaOH) and the pipet solution of 110 mM NaCl, 10 mM Na_2EGTA, 2 mM $MgCl_2$ and 2 mM $CaCl_2$ (pH 7.4, NaOH). The cells were illuminated with a diode-pumped solid-state laser (472 nm, 40 mW/mm^2, Pusch OptoTech GmbH, Germany).

RESULTS

Expression. Several variants of type I rhodopsins are found in *Oxyrrhis marina*.[4] Here, we further analyzed the most abundant rhodopsin,[4,5] which we named OR1 (Acc. No. ABV22426), with a high homology to known pR-like rhodopsins; to *Gloeobacter* rhodopsin (GR, ∼45% identity),[15] to XR (∼40%)[34] and to GPR (∼27%)[13] (see Figure S1 in the Supporting Information). The protein was expressed containing a C-terminal 9xHis-tag in the yeast *Pichia pastoris* under the control of the strong, methanol-inducible AOX promoter. OR1 was purified from a total membrane preparation by immobilized metal affinity chromatography. No contamination by other proteins could be detected on SDS gels (data not shown), and the 280/519 nm ratio, an indicator for rhodopsin purity, is ∼2. This value is in good agreement with a theoretical value of around 1.8 using an extinction coefficient of ∼43000 cm^{-1} M^{-1} that we determined from hydroxylamine treated samples.[35] The protein appears pink with an absorption maximum at 519 nm (Figure 1A) in accordance with the presence of L105, a known spectral tuning factor in GPR.[36] Strong expression could be already assessed during growth of the yeast cultures by the pink color of the membranes. On average, the protein yield amounted to ∼10−25 mg from 1 L of cell culture. We achieved ^{15}N-enrichment in OR1 in a defined medium as shown before for another type I rhodopsin,[37] giving access to NMR studies.

Isomer Composition and Solid-State NMR. The retinal isomer composition was determined from light- and dark-adapted samples. Their amounts were quantified after separation in normal-phase high-performance liquid chromatography. In contrast to bR, OR1 contains a larger fraction with an all-*trans* retinal already in the dark state with a ratio of 9:1 for all-*trans* to 13-*cis* isomers at pH 7.4 and did not show a light/dark adaption.[28] This result is in line with the solid-state NMR data on the ^{15}N-enriched protein. Figure 2 shows a ^{15}N CP-MAS NMR spectrum of OR1 reconstituted in DOPC. An excellent resolution is achieved indicating a rather homogeneous sample and/or favorable molecular dynamics of OR1 on the relevant NMR time scales (kHz). The resonance of the pSB is detected at 177.5 ppm with a relatively narrow line width (fwhh 0.6−0.9 ppm) indicating a prevailing all-*trans* conformer composition. A comparison with corresponding values from bR, GPR, model compounds and their correlations with λ_{max} (Figure 2 inset) shows that OR1 behaves more bR-like than for example GPR. The highly conserved single H62 shows two resonances from imidazole nitrogens: A protonated nitrogen is detected at 162.8 ppm, while a nitrogen atom with a free electron pair resonates at 241.6 ppm. The imidazole side chain of H62 is therefore in its uncharged form. For a protonated (charged) histidine side chain, we would only expect

dx.doi.org/10.1021/bi301412n | *Biochemistry* 2013, 52, 2750−2763

resonances between 160 and 170 ppm as in GPR under acidic conditions.[20] Unlike in GPR,[20] no indication for an H-bonding between H62 and the primary proton acceptor is found under our experimental conditions that would give rise to an additional resonance line.

pH Titration. pH titration experiments revealed reversible spectral changes in OR1 wild type which we compare to the spectrum of the mutant D100N that resides at the homologue position of the proton acceptor D97 in GPR (Figure 1A).[38] The removal of the negative charge close to the Schiff base proton leads to a bathochromic shift as known from other rhodopsins. In the case of the D100N, the maximum is at 562 nm compared to 519 nm of the wild type. This effect is more pronounced in OR1 than in other members as NpSRII[39] or GPR,[40] but comparable to blue pR (BPR)[36] and ESR.[26] The pH-induced changes in the wild type are furthermore sensitive toward the ionic strength and the added anion. Starting at neutral pH (species S_{ref}) and under salt-free conditions or low ionic strength conditions (0.1 M NaCl), lowering the pH increases the absorption at the red edge of the spectrum (~600 nm) without a significant change in the absorption maximum (Figure 1A/D/F). Our analysis was limited by the sample stability at low pH values. Incubation below pH 2.3 leads to irreversible changes of OR1 as followed by the formation of a species absorbing maximally at 418 nm. Hence we observe only the onset of a transition to a red-shifted protonated state (S_{600}) whose pK_a value should be less than ~3 as an upper limit. In the presence of 1 M NaCl, the spectral changes at 600 nm are already observed at higher pH values (Figure 1C/D) and a tentative pK_a for the S_{600} transition is shifted by almost one pK_a unit. In addition we can follow a second transition to a species absorbing maximally at 529 nm (Figure 1C). The assignment of two individual transitions is corroborated by the difference spectra compared to the one at neutral pH (S_{ref}), which are clearly distinguishable by their maxima (Figure 1B). The second transition to the S_{566} species is depicted in Figure 1F trailing the wavelength change of the absorbance maximum. For 1 M sodium chloride, it is described by a pK_a value of 3. Similar results are obtained in experiments with 1 M sodium sulfate although there are anion but not cation specific effects: The rise of the S_{600} species is not as strongly affected as in the case of sodium chloride (Figure 1D), and the maximum of the final species at low pH is lower ($\lambda_{max}[SO_4]$ = 526 nm vs $\lambda_{max}[Cl]$ = 530 nm, Figure 1F). So the main effect of the high ionic strength is the assessment of S_{566} formation at low pH that cannot be explained unambiguously: Either addition of salt could shift the pK_a value of a residue to higher values compared to the salt-free conditions (electrostatic coupling), or it is the binding of the salt itself that causes the spectral change.

How can we relate the spectral species to the protonation state of the D100 residue? It is obvious that the final spectrum at acidic pH (S_{566}) does not resemble the spectrum of the D100N mutant (Figure 1C/F). However, the induced changes by the S_{600} species might be tentatively assigned to a protonated D100, but only a minor fraction of the molecules would undergo this transition. The titration spectra of the D100N mutant which mimics the protonated acceptor further confirm our interpretation. Interestingly, a small red-shift (~13 nm) was observed in 0.1 M NaCl indicating protonation of groups other than D100 (Figure 1A). A similar behavior has been described for BPR.[36] In 1 M NaCl, the formation of S_{566} can be followed as in the wild type (Figure 1C). This sustains the existence of a second group different from D100 that only undergoes protonation in the presence of salt in the wild type and the D100N mutant. We think that the second protonation event is accompanied by full protonation of D100 in accordance with the spectrum of the D100N at pH 2.5 and the time-resolved kinetic experiments (see below).

In GPR and ESR, the pK_a value of the homologue of D100 is modulated by its interaction with the conserved histidine (H62 in OR1). Hence we inserted the mutation and followed the pH titration of the mutant bearing in mind if the D100N spectral features can be reproduced under acidic conditions similar to the corresponding H57M mutant in ESR.[26] Surprisingly, we observed a slight blue-shift in the spectrum albeit of the ionic conditions (Figure 1 E, F) when going from neutral pH 7.4 to pH 4 where we observed the biggest increase in the 600 nm absorbance for the wild type. Lowering the pH to 2 induces a similar red-shift in the mutant as in the wild type. The pK_a value of this transition and the wavelength of the absorbance maximum are again affected by the ionic conditions (Figure 1F), but both values are comparable to the wild type. In fact, the biggest difference is observed under salt-free conditions. The H62N mutation favors the build-up of a red-shifted species (comparable S_{566}) that is not observable under the same conditions in the wild type. Therefore, the modulating effect of the histidine residue is clearly different in OR1 compared to ESR or GPR.

The titration spectra can be summarized as follows: In the case of a stabilizing interaction of the protonated histidine with the deprotonated D100 as in ESR, we should observe an increase of the S_{600} species upon lowering the pH. A strong His-Asp cluster as in GPR can also be excluded on the basis of the low pK_a value of the spectral transitions observed in the wild type. For all shown variants, i.e., the wild type, the D100N and the H62N mutant, we observe the formation of a comparable S_{566} species at low pH. The differences are found in the salt requirement in the case for the wild type and the H62N mutant. That dependence is lost in the H62N mutant at least in the accessible pH range. Hence, the protonation state of this residue could affect the requirements for binding of anions that influence the spectral characteristics and the pK_a of D100 or the above-mentioned second group, but it does not strongly increase the pK_a of the S_{566} formation.

In the absence of chloride, measurements at the minimal accessible pH of 2.3 are complicated due to the existence of two initial states (S_{600}, protonated D100, and S_{ref}, deprotonated D100). Therefore the time-resolved spectroscopic measurements were performed at pH 2.5 in 1 M NaCl (S_{566}, Figure 1D, Figure 5E). Under these conditions the protein is still stable (no S_{418} species).

Pump−Probe Measurements. We investigated the isomerization process using the pump−probe technique. Figure 3 summarizes the temporal evolution of the spectral absorption features after photoexcitation of OR1 at pH 2.5 and pH 9. For pH 9, mainly 5 distinct spectral features can be identified. Around 450 nm a spectrally broad positive absorbance change is observed, which is caused by the excited state S_1 absorption (ESA; area A). At the red end of the probed spectral range (630−750 nm) the sample exhibits a negative difference band that is attributed to the stimulated emission (SE; area B). At around 520 nm a negative absorbance change can be seen that we assign to the ground state bleach (GSB; area C). The strong positive absorption feature from 560 to 640 nm is observed throughout the whole investigated time range and is composed of the ESA at early delay times and the photoproduct

dx.doi.org/10.1021/bi301412n | Biochemistry 2013, 52, 2750−2763

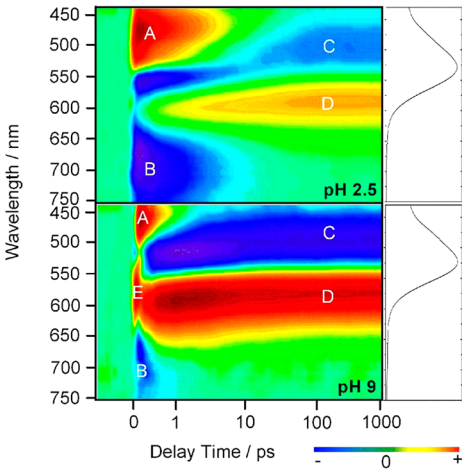

Figure 3. Time-resolved absorption changes after photoexcitation of OR1 at pH 2.5 (top) and pH 9 (bottom) with a 527 nm pulse (pH 2.5) and a 522 nm pulse (pH 9). The spectra are color-coded: red indicates positive, green zero and blue negative absorption. The time scale is linear until 1 ps and logarithmic from 1 ps to 1 ns. The ground-state spectra are shown on the right side. See text for details.

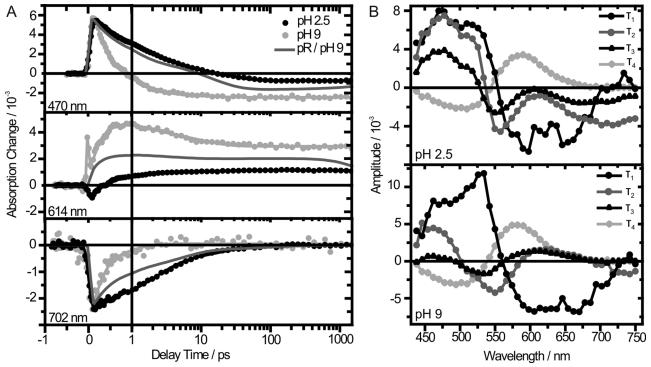

Figure 4. (A) Transient absorption change at pH 2.5 and pH 9. The solid line represents a sum of several exponential decays obtained by a global fit analysis. For comparison, the transient absorption change of GPR at pH 9 is shown. The data were taken from ref 55. (B) Decay associated spectra of the time constants obtained by the global fitting analysis for acidic and alkaline pH.

absorption (PA) at the end of the investigated time range (D). This species is the product state of the primary reaction and is supposed to be analogous to the K-intermediate in the photocycle of bR containing the isomerized retinal in its ground state. Moreover at pH 9, a positive absorption feature can be observed between 550 and 600 nm that lasts for several hundred femtoseconds (E). This signal can be attributed to a wave packet evolution on the S_1 potential energy surface. The latter is absent in the spectra of the wild type at pH 2.5. All other spectral features are conserved at this pH, although the dynamics are dramatically retarded.

For a better visualization of the pH effect on the primary reaction, single transients at characteristic wavelengths for both pH values are presented in Figure 4A. The overall decay of the spectral features is accelerated under alkaline conditions as reflected in the values for the time constants at pH 2.5 and 9 (Table 1). The corresponding DAS are depicted in Figure 4B. The first time constant τ_1 is similar for pH 2.5 and pH 9 and contains amplitudes in the region of the ESA and the SE region

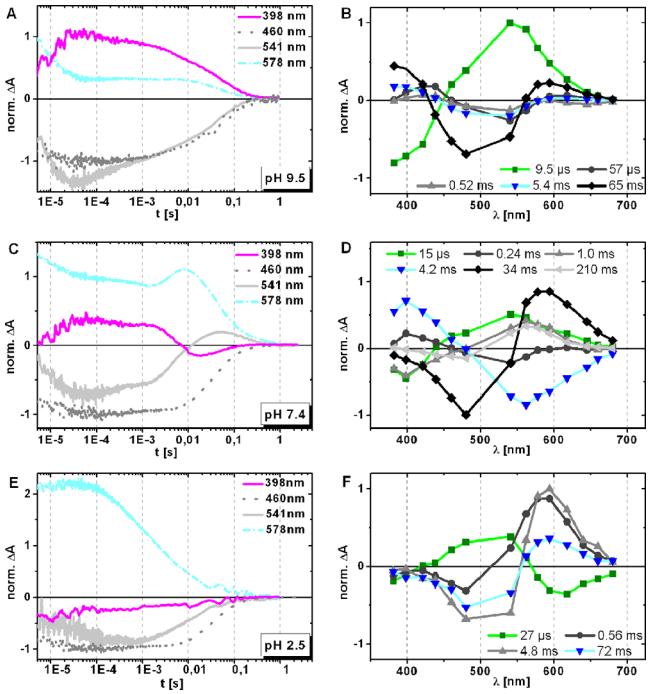

Figure 5. Light-induced absorption changes of OR1 under different pH conditions at 283 K. (A, C, E) Time course of spectral changes at characteristic wavelengths for the M-state (398 nm), the ground state bleaching (541 nm) and red-shifted states (578 nm) after flash excitation at 503 nm. The traces are normalized to the maximal amplitude of the 460 nm signal at pH 9.5 (A), pH 7.4 (C) and pH 2.5 (E), respectively. (B, D, F) Decay associated amplitude spectra derived from a global fit analysis for all 14 measured wavelengths at the selected pH values. The trace at 398 nm was smoothed by interpolation for clarity.

Table 1. Time Constants Obtained from a Global Fit Analysis of the Data from the Pump−Probe Measurements on OR1 in Comparison to Literature Data for GPR[a]

	τ_0/fs	τ_1/ps	τ_2/ps	τ_3/ps	τ_4
OR1 pH 2.5	<70	0.30 ± 0.03	2.1 ± 0.2	21 ± 2	∞
OR1 pH 7	<70	0.27	1.0	9.8	∞
OR1 pH 9	<70	0.27 ± 0.2	1.0 ± 0.1	9.5 ± 1	∞
D100N pH 7	<70	0.3 ± 0.03	2.2 ± 0.2	11 ± 1	∞
GPR pH 6[55]		0.15	1 ± 0.1	16 ± 1	∞
GPR pH 9[55]		0.14	0.3 ± 0.03	9.5 ± 1	∞
GPR D97N[40]		<0.2	1.4	20	

[a]The zeroth time constant contains coherent effects from the pump and the probe pulse, and only a higher limit is indicated.

and is therefore attributed to a wave packet motion on the S_1 potential energy surface.

The biggest spectral differences appear for the time constants τ_2 and τ_3. At pH 2.5 the spectra of both τ_2 and τ_3 show contributions of the ESA decay in the spectral range around 450 nm, the GSB recovery (550 nm), photoproduct formation and the SE decay. The high similarity of the spectra indicates that the underlying processes are identical and represent a biexponential decay of the excited state to the ground state. The spectral signature of τ_2 at pH 9 is similar to τ_2 at pH 2.5, whereas for τ_3 the contribution of the SE is lost, indicating that the excited state decays faster at alkaline pH. The spectra of the infinite time constant at both pH values resemble each other

dx.doi.org/10.1021/bi301412n | Biochemistry 2013, 52, 2750−2763

Table 2. Time Constants from the Global Fit Analysis of the Light-Induced Absorption Changes (Vis) at Three Different pH Values, the Thermodynamic Activation Parameters Determined from the Eyring Equation at pH 7.4 and the Comparison of the Spectroscopic Data with the Electrogenic Steps from the Analysis of the Voltage Signal[a]

		τ_1 [μs]	τ_2 [μs]	τ_3 [ms]	τ_4 [ms]	τ_5 [ms]	τ_6 [ms]
vis 283 K	pH 2.5	27 ± 2	560 ± 22	4.8 ± 0.2	72 ± 4		
	pH 7.4	15 ± 1	240 ± 32	1.0 ± 0.1	4.2 ± 0.2	34 ± 1	210 ± 8
	pH 9.5	8.6 ± 1	140 ± 5	2.9 ± 0.2	32 ± 4	94 ± 10	
vis pH 7.4	$\Delta H^{\ddagger}$ [kJ mol^{-1}]		86 ± 24	85 ± 6.4	63 ± 3.2	78 ± 1.8	56 ± 2
	$\Delta S^{\ddagger}$ [J K^{-1} mol^{-1}]		136 ± 83	111 ± 22	24 ± 11	58 ± 6.4	−35 ± 6.9
vis pH 7.4, 293 K (proteoliposomes)	τ_i	67			0.9	9.1	110
BLM, pH 7.4, 293 K	τ_i				1.0 ± 0.1	16± 2	10 ± 22
	rel amplitudes				0.31 ± 0.01	0.32 ± 0.02	0.37 ± 0.02

[a]The given standard errors derived from the global fit analysis.

and represent the difference absorption spectrum between the K-intermediate and the ground state.

Lowering the pH leads to the protonation of acid residues of the protein. For other proteins it is well-known that a negatively charged primary proton acceptor functions as an effective catalyst for photoisomerization.[41] Therefore we investigated the primary photodynamics of the OR1 D100N mutant (Figures S2 to S4 in the Supporting Information). The reaction dynamics are accelerated compared to wild type at pH 2.5 but are slower than wild type at pH 7 and 9. Remarkably, the primary photodynamics are not affected upon H62N mutation (Figures S5 and S6 in the Supporting Information), supporting the ssNMR data that there is no interaction between H62 and D100.[20]

Light-Induced Absorption Changes. The subsequent events of the photocycle were investigated by analyzing light-induced absorption changes with a time resolution of 5 μs at 283 K in detergent. As shown in Figure 5 and Table 2 we selected pH values with the proton acceptor D100 either in a protonated (pH 2.5, S_{566}) or in a deprotonated state (pH 9.5). Additionally, we included the data at pH 7.4 (S_{ref}) for comparison with the electrical measurements. The time course of the changes is depicted at wavelengths characteristic for the observed photointermediates, the deprotonated Schiff base (398 nm), the initial state (460 nm, 541 nm) and red-shifted intermediates (578 nm), respectively. The spectral properties of the photointermediates can be inferred from the DAS (Figure 5B/D/F) obtained from a global fit analysis. The corresponding time constants for the processes represent the transitions between the kinetic intermediates starting from P_1 to P_n.

At all measured pH values an early red-shifted intermediate, identical with P_1, is observed that is in accordance with the photoproduct of the isomerization from the pump−probe measurements (Figure 5A, 578 nm). At pH 9.5, our data show the decay of the K-like intermediate and the build-up of M-like state (τ_1) with a deprotonated Schiff base with a maximal absorption around 400 nm. The M-like intermediate and red-shifted intermediates persist over the whole time range. In analogy to bR, we term the latter ones the N-like and O-like intermediates. Reprotonation of the Schiff base and the recovery of the initial state occurs in several processes (τ_2 to τ_5). Hence, the kinetic intermediates P_2 to P_5 show contributions from several spectral species, the M-like and the N/O-like, respectively.

At pH 2.5 (initial state S_{566}), we could only detect red-shifted species. A deprotonated M-like intermediate was not observed comparable to the data from GPR[17] at pH 5 with a protonated primary acceptor. The red-shifted intermediate with a maximum at around 594 nm in the difference spectrum to the wild type rises in the microsecond time-range, whereas the decay to the ground state at pH 2.5 is a three-step process (τ_2−τ_4). Inspection of the time constants at different pH values reveals that the photocycle is slightly accelerated under alkaline and acidic conditions compared to neutral pH (Table 2).

Six time constants are needed to describe our data at pH 7.4. As at pH 9.5, only four spectral intermediates are present and describe the spectral characteristics of the kinetic intermediates P_1 to P_6. Starting again from the K-like intermediate (P_1), the M-like intermediate is formed in the microsecond to millisecond time range described by the process τ_1 to τ_3 (Figure 5D). Like at pH 9.5, the M-like state seems to equilibrate with other red-shifted intermediates that lead to a complex mixture of different spectral species for P_2 and P_3. The concentration of the M-state is strongly reduced compared to the data at pH 9.5. This behavior is similar to ESR.[26] In contrast to pH 9.5, the rise and the accumulation of a late red-shifted intermediate (N/O-like) can clearly be followed at 578 nm (Figure 5C) that is formed within a process described by a time constant of 4.2 ms (τ_4). The return to the ground state shows a biphasic behavior to the ground-state (τ_5 and τ_6). Additionally, the temperature dependence of the photocycle was measured between 283 and 308 K at pH 7.4 to further constrain the determination of the kinetic intermediates P_1 to P_6. The first time constant is not resolved at higher temperatures. Thus, we ignore τ_1. All other apparent rate constants follow an Arrhenius-like behavior, and their derived Eyring parameters are summarized in Table 2. The values for the enthalpy and entropy of activation are in a similar range as observed for other rhodopsins like bR.[29]

Environmental and Mutational Effects on the Photocycle. In reference to the titration data we use the presence of the M-state as an indicator for a deprotonated counterion, while its actual accumulation during the photocycle depends on the formation and decay rate. The assignment of D100 as the proton acceptor upon M-formation is supported by our mutant data. The rate of M-formation is speeded up in the D100E mutant similar to the homologue mutation in bR[42] (Figure S7 in the Supporting Information). Similar to the absence of the proton acceptor in the D100N mutant, we see no M-state at pH 2.5 and 1 M NaCl when starting the photocycle from S_{566} (Figure 5E). This is changed by any other condition where we always infer a mixture of initial states (S_{ref} and S_{600}) from the titration data and hence a fraction with a deprotonated proton

dx.doi.org/10.1021/bi301412n | Biochemistry 2013, 52, 2750−2763

acceptor, i.e., pH 4 with and without salt or pH 2.5 without salt (Figure 6A), although the effect seems to be different on the

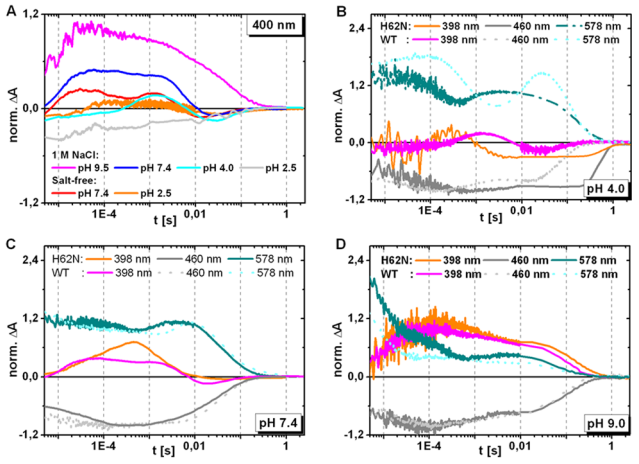

Figure 6. (A) The figure shows light-induced absorption changes at 400 nm of OR1 wild type at different pH values either in 1 M NaCl or in the absence of chloride ions. All spectra were normalized to ground-state bleaching at 460 nm and absorption. The traces at 398 nm have been smoothed for clarity using a Savitzky–Golay filter. (B–D) Light-induced absorption changes of the H62N mutant in presence of 1 M NaCl at pH 4 (B), 7.4 (C) and 9 (D) were compared to wild type of OR1. The spectra were normalized to 460 nm wavelength. The measurements at 398 nm were smoothed by interpolation.

rise of the M-state. Aside from the effect on the initial state, the ionic strength and the ion composition did not change the photocycle kinetics significantly (Figure 6A), leading to a comparable time course and to the presence of the same intermediates in the photocycle at pH 7.4 (Figure 6A) although the M-state is less populated in the absence of salt. So the light-induced absorbance changes agree with our titration data and the expected effect on the M-formation requiring a deprotonated proton acceptor in the initial state.

In ESR, the pH dependence of the M-state is strongly influenced by the conserved histidine. Therefore, we compared the light-induced changes between OR1 wild type and the H62N mutant (Figure 6 B–D). At pH 9.5, there is no significant difference between the two variants and we observe the same spectral intermediates in the H62N mutant as well. At pH 7.4, the photocycle time is accelerated compared to the wild type (66 ms vs 200 ms, Table S2 in the Supporting Information). A similar phenomenon has been described for GPR.[20,43] Furthermore, we detect a higher accumulation of the M-state in the mutant due to a faster rise during τ_2 (Table S2 and Figure S8 in the Supporting Information). At pH 4 the kinetics of M-rise and M-decay are faster than in the wild type. We detect only low levels of the M-state where we have for the initial states a fraction of the wild type molecules in S_{600} but only a slight blue shift for the H62N mutant. Hence, the H62N does not reveal the coupling between M-formation and the D100 spectral change as in the wild type. Furthermore, there is no drastic change in the pH dependence of the M-formation between wild type and H62N, i.e., no indication for a strong interaction between these two groups (Figure 6B–D).

OR1 Is a Proton Pump and Electrogenic Properties. The homology to bR and GPR and the presence of E111 at the proton donor position suggest OR1 to pump protons upon light activation. We followed up this question by patch-clamp recordings that reveal light-induced outward currents up to 300 pA (Figure 7A), i.e., proton transfer from the cytoplasm to the

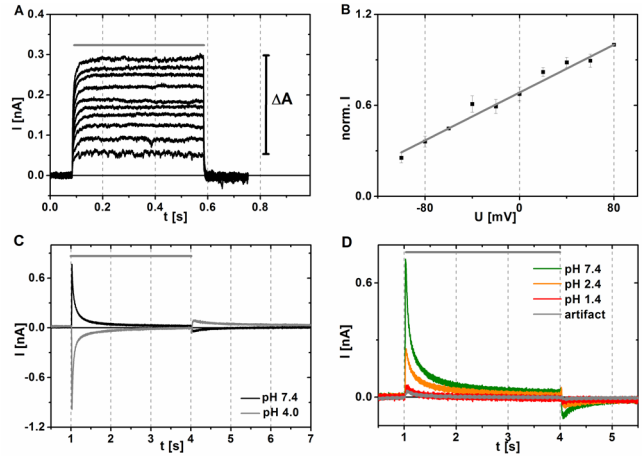

Figure 7. (A) Whole-cell patch-clamp experiments at pH 7.4 (n = 4) of NG108-15 cells expressing OR1-EYFP. The curves depict photocurrents upon illumination (472 nm, 40 mW/mm^2, gray bar) at holding potentials between −100 mV and +80 mV in Δ20 mV steps. The current density varied between 0.4 and 4.1 A/F indicating most probably varying OR1 concentrations in the plasma membrane. (B) Current–voltage relationship from patch-clamp recordings. (C) Control measurements with GPR at pH 7.4 and after changing to pH 4 upon illumination with a light filtered by 495 nm cutoff filter (gray bar). (D) Transient currents of OR1 after incubation at different pH values and 0.1 M NaCl in SSM experiments. The light-induced artifact on the gold surface is depicted as comparison.

extracellular side. At neutral pH, we observe a linear current–voltage relationship (Figure 7B) as known from other rhodopsins like bR[44] or GPR[22] with an apparent reversal potential of the pump current at −170 mV. This experiment proves the proton pumping activity of OR1, and it is further sustained by electrometric measurements with an artificial membrane bilayer system that selectively probes the nature of the transported ion by protonophores and the proton reactions at the pSB by the blue light effect (Figure S9 in the Supporting Information).

In a next step, we tested a change in the pump direction by pH variation as it has been assessed for GPR with a protonated proton acceptor at low pH.[18] Here, a solid supported membrane system (SSM)[33] allowed a solution exchange between the measurements. The amplitude of the peak current correlates with the proton transport activity. We used GPR as a reference and measured light-induced currents at pH 7.4 and pH 4 (Figure 7C) proving the change in the pump direction upon protonation of the proton acceptor D97.[22] Reconstituted OR1 adsorbed to a SSM-sensor generates currents up to 2 nA at pH 7.4. To control the stability of the system over time, the peak amplitude at pH 7.4 was used as a reference. A titration from pH 7.4 to pH 1.4 with 0.1 M NaCl as background decreased the amplitude of the signal to the level of the light artifact (Figure 7D). The effect was reversible, but we could not detect any change in the sign of the current at low pH even when the sample was incubated for more than ninety minutes. At pH 2.4 with S_{ref} and S_{600} as the initial states, only half of the charge was transported compared to pH 7.4 as calculated from the integral in Figure 7D. Hence, we still correlate this value to proton pumping activity of OR1 and not as the result of a transient deprotonation without a complete pumping cycle. In

dx.doi.org/10.1021/bi301412n | Biochemistry 2013, 52, 2750–2763

that case we would expect a highly diminished number of transported charges compared to pH 7.4.

To deduce the single proton transfer steps, we looked into the charge displacement that is associated with the individual transition of the intermediates. For the correlation with the spectral data, we performed time-resolved BLM measurements as described earlier[32] and measured the light-induced changes of OR1 reconstituted in proteoliposomes. Compared to the detergent conditions, the M-state formation is similar in proteoliposomes (Figure 8), although this process is described

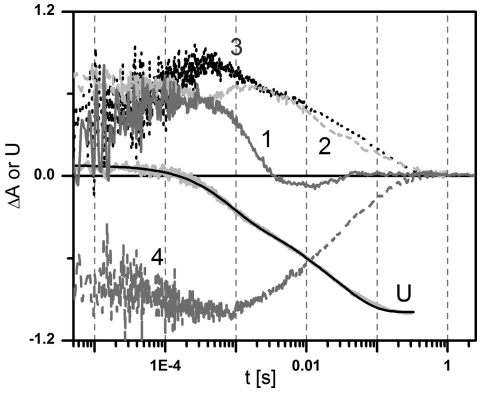

Figure 8. Comparison of light-induced absorption changes at 293 K and 0.1 M NaCl with voltage build-up from the BLM measurements (U) overlaid by a black line derived from a fit (see Table 2). The light-induced absorption changes were obtained from OR1 either in detergent [(1) 400 nm, smoothed with a Savitzky–Golay filter] or reconstituted in DOPC-liposomes [(2) 579 nm; (3) 400 nm; (4) 460 nm].

with a single time constant (τ_1 to τ_3 for detergent, Table 2) mainly because of the lower signal-to-noise ratio. On the millisecond time scale the M-state accumulates to higher concentration in proteoliposomes due to a slower reprotonation. A similar phenomenon has been observed for ESR[26] and GPR[45] and might be related to the surface pH of the liposomes. As shown in Figure 7 the electrogenic steps take place during the decay of the M-like intermediate (τ_4 = 1 ms) and decay of the N/O-like intermediate (τ_5 = 16 ms; τ_6 = 160 ms). In particular P_4–P_6 from the time-resolved spectroscopic data at pH 7.4 are mainly correlated with our obtained signal. The corresponding amplitudes reveal that all processes contribute equally to the electrogenicity of the proton transfer (Table 2). In contrast, the electrogenic steps in bR are associated to the rise and decay of the M-intermediate at neutral pH.[46] For OR1, the deprotonation of the Schiff base hardly contributes to its electrogenicity. Here, it is rather the reprotonation presumably from E111 and the reestablishment of the proton acceptor (D100, deprotonated) and the proton donor (E111, protonated). Furthermore, the results demonstrate that the photocycle and the associated proton transfer of OR1 are slow compared to bR.

DISCUSSION

Expression. We successfully expressed OR1 in *Pichia pastoris* and described its spectroscopic and functional behavior in detail by various spectroscopic and electrophysiological methods. Interestingly, the expression yields are exceptionally high compared to other membrane proteins expressed in *Pichia pastoris*.[47] In comparison, the protein yield for other type I rhodopsins ranges from 0.5 mg/L for wild type channelrhodopsin-2[48] up to 5 mg/L for some channelrhodopsin mutants or a rhodopsin from *Leptosphaeria maculans*.[37] For the latter protein, an isotope labeling protocol was already successfully demonstrated in *Pichia pastoris*. Here, we further provide support for using this host system to gain access to structural and functional studies of seven transmembrane helical receptors by NMR spectroscopy.[21,37,49]

Spectral Features. OR1 is a proton pump retaining structural and mechanistic properties of GPR and XR. A significant difference is found in the low pK_a value of the counterion below 3 in OR1. This reports changes in the electrostatic environment of the counterion D100. All the described experiments, the static and time-resolved spectroscopic measurements and the data from the charge transport experiments as well, are all in accordance with a pK_a-shift of the counterion to acidic pH (pK_a <3) compared to GPR (pK_a 7.7).[18] Therefore, the high pK_a value of the counterion is not a general feature of the pR family, as it can be seen from the comparison with the pK_a values from other members of this family and their decreasing order:

$$\mathbf{pR}(\sim 7)^{18} > \mathbf{XR}(\sim 6)^{50} > \mathbf{GR}(\sim 5)^{51} > \mathbf{OR1}(\leq 3) \sim \mathbf{ESR}^{26}$$

We have identified three spectral species in our titration measurements that set the basis for the kinetic experiments. Our reference state was defined at pH 7.4 with S_{ref} whose absorbance maximum is independent of the ionic conditions or of the presence of H62. At pH 7.4, the solid-state NMR experiments revealed H62 to be in a neutral state and the absence of hydrogen bonding interaction to this residue. By going to pH 9, we observe almost no spectral change and the photoisomerization rate followed in the pump–probe measurements is not altered reflecting a similar charge and geometrical arrangement of the chemical groups around the chromophore (see below). However, the amount of M-state formation strongly increases at alkaline pH that could be related to the coupling of the proton acceptor to another protonatable group. H62 increases M-formation at neutral pH, but shows qualitatively the same tendency as the wild type with a much higher accumulation of M at high pH (Figure 6B,C). Hence, the concentration of the M-state is not correlated to the charge of H62 in the initial state.

The titration of the D100 does not follow a simple titration curve and is furthermore complicated by its ionic strength sensitivity. Such a property is not unusual and has been described before for bR as the result of protonation of other residues.[52] The coupling of the counterion to a second ionizable group gains functional relevance in the proton transport mechanism as in bR, where counterion protonation lowers the pK_a of the proton release site,[53] or in ESR between the proton acceptor and the conserved histidine H57.[26] These phenomena are documented again in complex titration curves. Hereby, we infer also for OR1 that the spectral shift follows mainly the protonation state of the counterion itself. For OR1, we cannot describe the wild type and the mutant titration data in a minimal scheme with H62 and D100 as the protonation sites as going from S_{ref} to S_{600} (single protonated) and S_{566} (double protonated). The scheme is justified, because the absorbance at 600 nm decreases again (Figure 1D). If the D100N at neutral pH represents the single protonated species, we would expect a high accumulation of the same species in the

dx.doi.org/10.1021/bi301412n | *Biochemistry* 2013, 52, 2750–2763

titration of the H62N mutant. As this is not the case, other protonatable groups must be involved in the formation of the S_{566} species to explain the pH-dependency of the wild type. Still one has to be cautious about the conclusions from the mutant data because we do not know so far if the nature and the protonation state of the S_{566} species is identical in the mutants and in the wild type. Further experiments that follow the charge state of the H62 in the wild type and the D100N could help for an unambiguous assignment. The small spectral changes at pH 2.4 (0 M NaCl) are in contrast to the clear shift of the absorbance maximum of the D100N mutant ($\Delta e \sim 0.2$ eV; λ_{max} = 562 nm). This could be simply the result from a much lower pK_a value of D100 in the wild type leading to the low accumulation of S_{600} under the accessible conditions. With S_{ref} and the D100N as principal components, we would estimate a fraction of less than 30% of the molecules. Such a notion would be in line with the presence of the M-state in the light-induced absorption changes at pH 2.5 in salt-free conditions (Figure 6A) and the charge transport measurements (Figure 7).

The presence of chloride increases the pK_a value of D100 (S_{600} formation). As we observe the same spectral species devoid of the chloride ion, we do not assume a tight binding of chloride close to the retinal, e.g., to D100 itself. Instead, chloride ions (and to a lesser extent sulfate ions) could modulate the interaction between D100 and further groups in OR1 either by binding to the group alone or as HCl. As a result, we could not find conditions with the S_{600} as dominant initial state. However, the spectral shift and the decrease in M-formation argue for a fractional protonation of the proton acceptor in this species. The location of the D100 and the phenotype of the D100N and D100E mutant provide arguments for its assignment as the proton acceptor.

The H62 could be involved in the formation of the S_{600} as mutating the residue abolishes its accumulation. Therefore, one could speculate about a protonation state of OR1 where one proton is shared between H62 and D100 as it has been suggested for XR[50] and demonstrated for GPR.[20] Instead of populating S_{600} by further decreasing the pH, a second protonation reaction arises as assessed by the formation of S_{566}. The mutant D100N undergoes the same salt and pH-dependent transition to S_{566} (Figure 1A,C), so that other protonatable groups in addition to D100 must be involved in the wild type and in the D100N mutant in the formation of this species. Prime candidates would be other residues involved in the complex counterion formation like the homologue residue D212 in bR—whose chloride-dependent protonation reaction causes the formation of the so-called acid purple species[54]—but not the conserved histidine H62 in OR1 that still forms S_{566}. In S_{566}, the proton acceptor D100 is fully protonated as we see no M-formation and a retarded photoisomerization rate.

In ESR, the presence of the homologue histidine (H57) stabilizes the deprotonated state of the counterion whose protonation can only be followed at pH values below 3.[26] The removal of the histidine shifts the pK_a value to 6.3 and reestablishes the same spectral features as in the proton acceptor mutant D85N. Our results are in clear contrast and reveal another variation of the histidine theme in the pR family. The behavior of the H62N mutant does not support a strong interaction between the histidine and the proton acceptor in the initial state, because the spectral transition to the S_{566} occurs at low pK_a values under any ionic condition (Figure 1F), i.e., the pK_a of the proton acceptor remains low independent of the conserved histidine. Also the salt sensitivity of the pK_a for the S_{566} transition is comparable to that of the wild type, so that we do not assume H62 to be part of the salt binding site.

Ultrafast Spectroscopy. Pump−probe spectroscopy records the primary reaction step in the photocycle of OR1, e.g., the photoisomerization and the formation of the K-like intermediate. In the global fit analysis, five time constants were necessary to approximate the transient data set (Table 1). The time constant τ_0 is lower than the time resolution of the laser system and is therefore not further considered. The time constants τ_1−τ_4 can be compared to the ones found for GPR reported earlier[55] and are attributed to the following processes: After photon absorption the retinal in its all-*trans* conformation is excited to the first excited electronic state (S_1). The first time constant τ_1 can be assigned to the motion of the initially prepared wave packet out of the Franck−Condon region. The propagation on the multidimensional energy surface includes several retinal stretching followed by torsional modes (τ_2) leading to the S_1/S_0 conical intersection with the electronic ground state (τ_2, τ_3), where one double bond is twisted by 90°.[56,57] For GPR it was postulated that a part of the excited state population will not reach the CI directly, but end up in a state on the S_1 potential energy surface separated from the CI by an energetic barrier (τ_3). They can access the CI on a picosecond time scale.[19] For OR1 this mechanism is plausible for pH 2.5 but is not valid for pH 9, since the DAS of τ_3 lacks of contribution from SE. Therefore this time constant must be attributed to processes occurring on the S_0 surface. After reaching the CI the reaction path splits into two channels, where the molecules can adopt either the all-*trans* or the 13-*cis* conformation, which is called the K-intermediate.

As in GPR,[19] the primary photodynamics of OR1 are strongly accelerated by increasing the pH. This behavior is most likely caused by changed electrostatics associated with an altered hydrogen-bonding network. A key factor is the protonation state of the primary proton acceptor: It is assumed that the first excited electronic state of retinal proteins exhibits a polar character. In comparison to the electronic charge distribution in the ground state, the photoexcitation moves partial positive charge toward the hydrocarbon tail of the chromophore.[58] An immediate change in dipole moment by 12 D upon photoexcitation causes a polarization of the retinal in bR.[59,60] The partial positive charge can be stabilized by negatively charged amino acids near the C13 position of the retinal. As a result the double bond character is reduced at this position and therefore the energy barrier for isomerization is decreased.[61] Furthermore a negatively charged primary proton acceptor is known to affect the nature of the S_1 potential energy surface, leading to a deeper slope toward the CI.[62] The necessity of a negatively charged primary proton acceptor for fast isomerization is illustrated by the observation that the primary dynamics is also slowed down upon D100N mutation. The primary photodynamics of OR1 D100N is more similar to OR1 at pH 2.5 than to OR1 at the same pH, e.g., a retarded photoisomerization rate and a biexponential decay of the S_1 state (Figure S4 in the Supporting Information) that are properties also found in other rhodopsins like bR or GPR (Table 1, Table S1 in the Supporting Information). However, the reaction mechanism for OR1 D100N is accelerated compared to OR1 at pH 2.5. Taking into account that the absorption maximum is more red-shifted for OR1 D100N (λ_{Max} = 562 nm) than for OR1 at pH 2.5 (λ_{Max} = 529 nm) suggests that either there are conformational changes within the retinal binding pocket for OR1 D100N or other groups are

dx.doi.org/10.1021/bi301412n | *Biochemistry* 2013, 52, 2750−2763

additionally protonated in the wild type at pH 2.5 as speculated in the titration data for S_{566}. This would also explain the altered dynamics found for OR1 D100N and OR1 at pH 2.5, although both species exhibit a neutral primary proton acceptor. The D100N mutant was not stable at low pH to assess differences between the mutant and the wild type at low pH when both variants have undergone the transition to S_{566}.

Although the overall transient absorption spectra in Figure 3 look similar to GPR reported earlier, there are significant differences: The time constants given in Table 1 may suggest a faster decay for the primary reaction of GPR compared to OR1, and the fast component (τ_2) is more pronounced in OR1, leading to a faster overall reaction dynamics as indicated in Figure 4, where individual transients for OR1 and GPR are compared. Moreover, the DAS of τ_3 exhibit no contribution to the stimulated emission suggesting a single-exponential decay of the S_1 state for OR1. In contrast to this a biexponential decay was observed for pH 2.5. A similar behavior was also reported for bR (see Table S1 in the Supporting Information), although the time constant of the single-exponential decay of the S_1 state is 2-fold slower for OR1 at alkaline pH compared to bR. For GPR a contribution to SE is observed for τ_2 and τ_3 at pH 6 and pH 9, suggesting a biexponential decay for both pH values. The reaction rate and the underlying mechanism strongly depend on the nature of the S_1 potential energy surface. Quantum mechanical calculation reveals that the shape of the S_1 surface is mainly determined by the relative orientation of acidic side chains of the complex counterion toward the Schiff base.[62] Therefore our data suggest that the stabilization of the protonated Schiff base through coordination with the complex counterion is unique for OR1.

With respect to the role of the conserved histidine, a comparison of pump−probe measurements of GPR wild type and H75N reveals the strong dependence of the photoisomerization rate on the protonation state of D97.[20] Its pK_a is lowered upon H75N mutation, and the rate of photoisomerization is affected as well. For OR1 it was found that the pK_a is unaffected upon H62N mutation. Therefore the primary photodynamics are similar for OR1 wild type and H62N (Figures S5 and S6 in the Supporting Information), indicating the absence of the His-Asp cluster OR1 at physiological pH in accordance with the solid-state NMR data.

Light-Induced Absorption Changes and Electrometric Measurements. Besides the K-like state, the deprotonated Schiff base (M-like) and late red-shifted intermediates (N- and O-like) are detected. So far, we cannot clearly discriminate between the N-state (relaxed 13-*cis* retinal and deprotonated E111) and the O-state (all-*trans* retinal and protonated E111). The presence of the N-like state is mainly a consequence of the different accumulation of the O-like state at pH 7.4 and pH 9.5 (Figure 5A/C). Furthermore the absorbance changes exhibit a strong pH-dependence which can be best pursued by comparing the course of deprotonated species at different pH's (Table 2, Figure 5 and Figure 6A). Especially, the high accumulation of the M-state at high pH is noteworthy. Although the deprotonation of the Schiff base occurs at pH 7.4 and pH 9.5 with nearly the same kinetics (τ_1 ~10 μs), the amplitude of the deprotonated species is significantly higher at pH 9.5. Therefore the interaction between the Schiff base and the counterion seems to be influenced by a protonatable group at alkaline pH that leads to the stabilization of the neutral complex as suggested for ESR.[26] Here, it was suggested that the conserved histidine is the responsible factor. However, we could show that H62 is already neutral at pH 7.4 (Figure 2) although we cannot fully rule out effects of the lipid environment in the solid-state NMR data compared to the detergent micelles. Indications might come from the transient absorbance measurements (Figure 8) that depict a slower reprotonation of the SB. In ESR, it shifted the pK_a of the histidine by two pK units. Titration experiments on OR1 reconstituted in liposomes were qualitatively similar for the S_{600} and S_{566} transitions (data not shown), but so far we cannot assess the effect directly on H62.

Moreover, the amplitude spectra reveal that at pH 7.4 the second build-up of deprotonated species (τ_3) and the reprotonation of the Schiff Base (τ_4) display the main pH-dependent changes to pH 9.5 (τ_3). As for the titration, we could speculate about the influence of another pH sensitive group coupled to the protonation state of the proton acceptor leading to either a splitting of the photocycle or the presence of two differently protonated initial states with two photocycles. Interestingly, the H62N exerts its strongest effect at pH 7.4 on the multiphasic M-rise in the wild type, thereby accelerating the second build-up of the deprotonated species. As for the titration data, the histidine has a modulating effect on the primary proton acceptor also during the photocycle that seems to be not coupled to the protonation of H62. The effect would be the stabilization of the neutral SB and counterion complex (M-state) either by the altered electrostatics, by a different hydrogen-bonding network or by affecting the reprotonation rate from an internal proton donor. This property continues to be present during the reprotonation of the SB affecting the amplitude of the N-/O-like intermediates getting more accumulated at pH 7.4. Apparently, the photocycle—especially at pH 7.4—reveals even more complexity than as described in a linear photocycle. Thus, additional experiments (e.g., time-resolved vibrational spectroscopy) have to be performed to get deeper insights to the complex behavior of OR1.

In the electrometric measurements, we show the linkage between the photocycle and vectorial proton transport with its main electrogenic steps for OR1 (Figure 8) mainly coupled to the reprotonation. We observe a very fast positive offset in our potential signal that is often observed during the K-state in rhodopsins. Interestingly, we could not detect a big electrogenicity upon deprotonation of the SB that is different to GPR when measured in cell suspensions,[63] but similar to *in vitro* current measurements.[38] The reprotonation of the Schiff base occurs with τ_4 (~1 ms) while τ_5 and τ_6 are coupled to the decay of the N/O-like intermediate of OR1 and show the reprotonation of E111 and proton release to the extracellular surface. Therefore the sequence of the protonation reactions is similar to other members of the pR family. In GR and GPR, experiments with the pH-sensitive dye pyranine revealed a preceding uptake of a proton before the release of a proton to the extracellular side. Those reactions were also coupled to the N/O-like intermediates.[15,17] The altered behavior compared to bR was explained with a different proton release group (E194 and E204 in bR) that is absent in the pR family and the cause for fast proton release in bR.

Role of H62 and Biological Function. The conserved histidine is an indicative sequence marker for the pR family. Its function seems to be diverse and context sensitive. In GPR, the His-Asp cluster forms a pH-dependent hydrogen bond shifting the pK_a of the proton acceptor to high values.[20] In contrast for ESR, the interaction stabilizes the deprotonated state of the proton acceptor in the initial state and during the photocycle.[26]

dx.doi.org/10.1021/bi301412n | *Biochemistry* 2013, 52, 2750−2763

Here for OR1, we see only a minor effect on the proton acceptor. OR1 has a more similar phenotype in its titration behavior than, e.g., bR while it shows a stronger pH dependence of its M-formation and M-decay. But this observation seems not to be solely correlated to the charge state of the histidine. This is in accordance to the previous reports stating that the histidine is not necessary for proton pumping or the sole factor for the high pK_a.[20] Therefore, the role of the histidine in OR1 might rather be related to the kinetic modulation of proton transfer steps and here especially with a coupling to the so far unknown proton release group in the pR family.

Oxyrrhis marina is a heterotrophic organism. Still, strong expression of OR1 is observed in *Oxyrrhis* cells, which raises the question about the rhodopsin's role under physiological conditions. As described in the introduction, part a phototrophic[4] as well as a phototactic function have been proposed by two independent studies.[5] Our results with low pK_a value of the counterion, pump activity and charge translocation over a wide pH range would clearly suggest a general involvement in energy fixation. Initial patch-clamp data (Figure 7 A,B) clearly demonstrated the light-induced pumping of OR1. Interestingly, the titration data from the electrometric measurements (Figure 6 D) indicates that vectorial proton transport is not reversed even under very acidic conditions. This is in clear contrast to GPR,[18,22] but again similar to ESR,[26] reflecting the different environment at the pSB in different pRs. Therefore the low pK_a value of the counterion would guarantee OR1 to pump protons into an acidified compartment as proposed as possible function by Slamovits et al.. A McpT-like sensor, which detects the change in membrane potential generated by OR1 as known from *Halobacterium salinarium* for bR,[64] could be one possible explanation for OR1's phototactic activity. Furthermore the strong expression of OR1 *in vivo* might result in the presence of the rhodopsin in internal compartment and in a small fraction also in the plasma membrane enabling phototaxis. A second minor group of rhodopsins found in *Oxyrrhis marina* are bR-like proteins, suggesting as well a role in energy fixation. It is not known whether both rhodopsin genes are encoded in the same strain or not. But the fact that both seem to be involved in the energy metabolism of the cell makes it unlikely that a combination of both proteins in the dinoflagellate could explain the contradictory results.

In conclusion, we presented an initial characterization from a eukaryotic member of the pR family. OR1 acts as a proton pump within a broad pH range whose pumping cycle is connected to a bR-like photocycle. The conserved histidine residue shows enigmatic features that have to be addressed more specifically with spectroscopic techniques.

■ ASSOCIATED CONTENT

Supporting Information

Further experimental results (Tables S1 and S2 and Figures S1−S9). This material is available free of charge via the Internet at http://pubs.acs.org.

■ AUTHOR INFORMATION

Corresponding Author

*Max-Planck-Institut für Biophysik, Abteilung für Biophysikalische Chemie, Max-von-Laue Strasse 3, 60438 Frankfurt am Main, Germany. Phone: ++49-69-63032007. Fax: ++49-69-63032222. E-mail: christian.bamann@biophys.mpg.de.

Funding

This work was supported by the Max Planck Society, the DFG (Sonderforschungsbereich 807 to J.W., C.G. and E.B.) and the Center of Excellence Frankfurt Macromolecular Complexes.

Notes

The authors declare no competing financial interest.

■ ACKNOWLEDGMENTS

We thank Dr. Katrin Feldbauer (MPI) and Dr. Mirka-Kristin Verhoefen (JWG) for critical reading of the manuscript. We would like to thank Dr. Ionela Radu (Freie Universität Berlin) for discussions and access to unpublished data. Furthermore the authors thank Dr. Christine Keipert for support with the SURFE^{2}R-System. Additionally we would like to thank Helga Husmann for her help in the figure preparation, Stefan Geys for support with NG108-15 cells and Heike Biehl for excellent technical support.

■ ABBREVIATIONS USED

OR1, *Oxyrrhis marina* rhodopsin; bR, bacteriorhodopsin; GR, gloeobacter rhodopsin; GPR, green proteorhodopsin; pR, proteorhodopsin; sR, sensory rhodopsin; BLM, black lipid membrane; RT, room temperature; SSM, solid supported membrane; XR, xanthorhodopsin; DAS, decay-associated spectra; MAS, magic angle spinning; pSB, protonated Schiff base; ESR, rhodopsin from *Exiguobacterium sibiricum*

■ REFERENCES

(1) Montagnes, D. J. S., Lowe, C. D., Roberts, E. C., Breckels, M. N., Boakes, D. E., Davidson, K., Keeling, P. J., Slamovits, C. H., Steinke, M., Yang, Z., and Watts, P. C. (2011) An introduction to the special issue: Oxyrrhis marina, a model organism? *J. Plankton Res. 33*, 549−554.

(2) Gao, X. P., and Li, J. Y. (1986) Nuclear division in the marine dinoflagellate Oxyrrhis marina. *J. Cell Sci. 85*, 161−175.

(3) Slamovits, C. H., and Keeling, P. J. (2011) Contributions of Oxyrrhis marina to molecular biology, genomics and organelle evolution of dinoflagellates. *J. Plankton Res. 33*, 591−602.

(4) Slamovits, C. H., Okamoto, N., Burri, L., James, E. R., and Keeling, P. J. (2011) A bacterial proteorhodopsin proton pump in marine eukaryotes. *Nat. Commun. 2*, 183.

(5) Hartz, A. J., Sherr, B. F., and Sherr, E. B. (2011) Photoresponse in the Heterotrophic Marine Dinoflagellate Oxyrrhis marina. *J. Eukaryotic Microbiol. 58* (2), 171−177.

(6) Frigaard, N. U., Martinez, A., Mincer, T. J., and DeLong, E. F. (2006) Proteorhodopsin lateral gene transfer between marine planktonic Bacteria and Archaea. *Nature 439*, 847−850.

(7) Nagel, G., Ollig, D., Fuhrmann, M., Kateriya, S., Musti, A. M., Bamberg, E., and Hegemann, P. (2002) Channelrhodopsin-1: a light-gated proton channel in green algae. *Science 296*, 2395−2398.

(8) Tsunoda, S. P., Ewers, D., Gazzarrini, S., Moroni, A., Gradmann, D., and Hegemann, P. (2006) H+-pumping rhodopsin from the marine alga Acetabularia. *Biophys. J. 91*, 1471−1479.

(9) Waschuk, S. A., Bezerra, A. G., Shi, L., and Brown, L. S. (2005) Leptosphaeria rhodopsin: Bacteriorhodopsin-like proton pump from a eukaryote. *Proc. Natl. Acad. Sci. U.S.A. 102*, 6879−6883.

(10) Sineshchekov, O. A., Jung, K. H., and Spudich, J. L. (2002) Two rhodopsins mediate phototaxis to low- and high-intensity light in Chlamydomonas reinhardtii. *Proc. Natl. Acad. Sci. U.S.A. 99*, 8689−8694.

(11) Jung, K.-H. (2007) The Distinct Signaling Mechanisms of Microbial Sensory Rhodopsins in Archaea, Eubacteria and Eukarya. *Photochem. Photobiol. 83*, 63−69.

(12) Oesterhelt, D., and Stoeckenius, W. (1971) Rhodopsin-like protein from the purple membrane of Halobacterium halobium. *Nat. New Biol. 233*, 149−152.

(13) Beja, O., Aravind, L., Koonin, E. V., Suzuki, M. T., Hadd, A., Nguyen, L. P., Jovanovich, S. B., Gates, C. M., Feldman, R. A., Spudich, J. L., Spudich, E. N., and DeLong, E. F. (2000) Bacterial Rhodopsin: Evidence for a New Type of Phototrophy in the Sea. *Science 289*, 1902−1906.
(14) Fuhrman, J. A., Schwalbach, M. S., and Stingl, U. (2008) Proteorhodopsins: an array of physiological roles? *Nat. Rev. Microbiol. 6*, 488−494.
(15) Miranda, M. R. M., Choi, A. R., Shi, L. C., Bezerra, A. G., Jung, K. H., and Brown, L. S. (2009) The Photocycle and Proton Translocation Pathway in a Cyanobacterial Ion-Pumping Rhodopsin. *Biophys. J. 96*, 1471−1481.
(16) Luecke, H., Schobert, B., Stagno, J., Imasheva, E. S., Wang, J. M., Balashov, S. P., and Lanyi, J. K. (2008) Crystallographic structure of xanthorhodopsin, the light-driven proton pump with a dual chromophore. *Proc. Natl. Acad. Sci. U.S.A. 105*, 16561−16565.
(17) Dioumaev, A. K., Brown, L. S., Shih, J., Spudich, E. N., Spudich, J. L., and Lanyi, J. K. (2002) Proton transfers in the photochemical reaction cycle of proteorhodopsin. *Biochemistry 41*, 5348−5358.
(18) Friedrich, T., Geibel, S., Kalmbach, R., Chizhov, I., Ataka, K., Heberle, J., Engelhard, M., and Bamberg, E. (2002) Proteorhodopsin is a light-driven proton pump with variable vectoriality. *J. Mol. Biol. 321*, 821−838.
(19) Huber, R., Kohler, T., Lenz, M. O., Bamberg, E., Kalmbach, R., Engelhard, M., and Wachtveitl, J. (2005) pH-dependent photoisomerization of retinal in proteorhodopsin. *Biochemistry 44*, 1800−1806.
(20) Hempelmann, F., Holper, S., Verhoefen, M. K., Woerner, A. C., Kohler, T., Fiedler, S. A., Pfleger, N., Wachtveitl, J., and Glaubitz, C. (2011) His75-Asp97 Cluster in Green Proteorhodopsin. *J. Am. Chem. Soc. 133* (12), 4645−4654.
(21) Reckel, S., Gottstein, D., Stehle, J., Lohr, F., Verhoefen, M. K., Takeda, M., Silvers, R., Kainosho, M., Glaubitz, C., Wachtveitl, J., Bernhard, F., Schwalbe, H., Guntert, P., and Dotsch, V. (2011) Solution NMR structure of proteorhodopsin. *Angew. Chem., Int. Ed. 50*, 11942−11946.
(22) Lörinczi, É., Verhoefen, M.-K., Wachtveitl, J., Woerner, A. C., Glaubitz, C., Engelhard, M., Bamberg, E., and Friedrich, T. (2009) Voltage- and pH-Dependent Changes in Vectoriality of Photocurrents Mediated by Wild-type and Mutant Proteorhodopsins upon Expression in Xenopus Oocytes. *J. Mol. Biol. 393*, 320−341.
(23) Dioumaev, A. K., Wang, J. M., Balint, Z., Varo, G., and Lanyi, J. K. (2003) Proton transport by proteorhodopsin requires that the retinal Schiff base counterion Asp-97 be anionic. *Biochemistry 42*, 6582−6587.
(24) Yoshizawa, S., Kawanabe, A., Ito, H., Kandori, H., and Kogure, K. (2012) Diversity and functional analysis of proteorhodopsin in marine Flavobacteria. *Environ. Microbiol. 14* (5), 1240−1248.
(25) Martinez, A., Bradley, A. S., Waldbauer, J. R., Summons, R. E., and DeLong, E. F. (2007) Proteorhodopsin photosystem gene expression enables photophosphorylation in a heterologous host. *Proc. Natl. Acad. Sci. U.S.A. 104*, 5590−5595.
(26) Balashov, S. P., Petrovskaya, L. E., Lukashev, E. P., Imasheva, E. S., Dioumaev, A. K., Wang, J. M., Sychev, S. V., Dolgikh, D. A., Rubin, A. B., Kirpichnikov, M. P., and Lanyi, J. K. (2012) Aspartate-histidine interaction in the retinal schiff base counterion of the light-driven proton pump of Exiguobacterium sibiricum. *Biochemistry 51*, 5748−5762.
(27) Larkin, M. A., Blackshields, G., Brown, N. P., Chenna, R., McGettigan, P. A., McWilliam, H., Valentin, F., Wallace, I. M., Wilm, A., Lopez, R., Thompson, J. D., Gibson, T. J., and Higgins, D. G. (2007) Clustal W and Clustal X version 2.0. *Bioinformatics 23*, 2947−2948.
(28) Scherrer, P., Mathew, M. K., Sperling, W., and Stoeckenius, W. (1989) Retinal isomer ratio in dark-adapted purple membrane and bacteriorhodopsin monomers. *Biochemistry 28*, 829−834.
(29) Chizhov, I., Chernavskii, D. S., Engelhard, M., Mueller, K. H., Zubov, B. V., and Hess, B. (1996) Spectrally silent transitions in the bacteriorhodopsin photocycle. *Biophys. J. 71*, 2329−2345.
(30) Helbing, J., Bregy, H., Bredenbeck, J., Pfister, R., Hamm, P., Huber, R., Wachtveitl, J., De Vico, L., and Olivucci, M. (2004) A fast photoswitch for minimally perturbed peptides: investigation of the trans → cis photoisomerization of N-methylthioacetamide. *J. Am. Chem. Soc. 126*, 8823−8834.
(31) Wilhelm, T., Piel, J., and Riedle, E. (1997) Sub-20-fs pulses tunable across the visible from a blue-pumped single-pass noncollinear parametric converter. *Opt. Lett. 22*, 1494−1496.
(32) Ruitenberg, M., Kannt, A., Bamberg, E., Ludwig, B., Michel, H., and Fendler, K. (2000) Single-electron reduction of the oxidized state is coupled to proton uptake via the K pathway in Paracoccus denitrificans cytochrome c oxidase. *Proc. Natl. Acad. Sci. U.S.A. 97*, 4632−4636.
(33) Pintschovius, J., and Fendler, K. (1999) Charge translocation by the Na+/K+-ATPase investigated on solid supported membranes: rapid solution exchange with a new technique. *Biophys. J. 76*, 814−826.
(34) Balashov, S. P., Imasheva, E. S., Boichenko, V. A., Anton, J., Wang, J. M., and Lanyi, J. K. (2005) Xanthorhodopsin: a proton pump with a light-harvesting carotenoid antenna. *Science 309*, 2061−2064.
(35) Scharf, B., Hess, B., and Engelhard, M. (1992) Chromophore of sensory rhodopsin II from Halobacterium halobium. *Biochemistry 31*, 12486−12492.
(36) Wang, W. W., Sineshchekov, O. A., Spudich, E. N., and Spudich, J. L. (2003) Spectroscopic and photochemical characterization of a deep ocean proteorhodopsin. *J. Biol. Chem. 278*, 33985−33991.
(37) Fan, Y., Shi, L., Ladizhansky, V., and Brown, L. (2011) Uniform isotope labeling of a eukaryotic seven-transmembrane helical protein in yeast enables high-resolution solid-state NMR studies in the lipid environment. *J. Biomol. NMR 49*, 151−161.
(38) Varo, G., Brown, L. S., Lakatos, M., and Lanyi, J. K. (2003) Characterization of the photochemical reaction cycle of proteorhodopsin. *Biophys. J. 84*, 1202−1207.
(39) Verhoefen, M. K., Lenz, M. O., Amarie, S., Klare, J. P., Tittor, J., Oesterhelt, D., Engelhard, M., and Wachtveitl, J. (2009) Primary reaction of sensory rhodopsin II mutant D75N and the influence of azide. *Biochemistry 48*, 9677−9683.
(40) Verhoefen, M. K., Neumann, K., Weber, I., Glaubitz, C., and Wachtveitl, J. (2009) Primary reaction dynamics of proteorhodopsin mutant D97N observed by femtosecond infrared and visible spectroscopy. *Photochem. Photobiol. 85*, 540−546.
(41) Scholz, F., Bamberg, E., Bamann, C., and Wachtveitl, J. (2012) Tuning the Primary Reaction of Channelrhodopsin-2 by Imidazole, pH, and Site-Specific Mutations. *Biophys. J. 102*, 2649−2657.
(42) Butt, H. J., Fendler, K., Bamberg, E., Tittor, J., and Oesterhelt, D. (1989) Aspartic acids 96 and 85 play a central role in the function of bacteriorhodopsin as a proton pump. *EMBO J. 8*, 1657−1663.
(43) Bergo, V. B., Sineshchekov, O. A., Kralj, J. M., Partha, R., Spudich, E. N., Rothschild, K. J., and Spudich, J. L. (2009) His-75 in Proteorhodopsin, a Novel Component in Light-driven Proton Translocation by Primary Pumps. *J. Biol. Chem. 284*, 2836−2843.
(44) Nagel, G., Kelety, B., Mockel, B., Buldt, G., and Bamberg, E. (1998) Voltage dependence of proton pumping by bacteriorhodopsin is regulated by the voltage-sensitive ratio of M1 to M2. *Biophys. J. 74*, 403−412.
(45) Krebs, R. A., Alexiev, U., Partha, R., DeVita, A. M., and Braiman, M. S. (2002) Detection of fast light-activated H+ release and M intermediate formation from proteorhodopsin. *BMC Physiol. 2*, 5.
(46) Heberle, J., and Dencher, N. A. (1992) Surface-bound optical probes monitor protein translocation and surface potential changes during the bacteriorhodopsin photocycle. *Proc. Natl. Acad. Sci. U.S.A. 89*, 5996−6000.
(47) Macauley-Patrick, S., Fazenda, M. L., McNeil, B., and Harvey, L. M. (2005) Heterologous protein production using the Pichia pastoris expression system. *Yeast 22*, 249−270.
(48) Bamann, C., Kirsch, T., Nagel, G., and Bamberg, E. (2008) Spectral Characteristics of the Photocycle of Channelrhodopsin-2 and Its Implication for Channel Function. *J. Mol. Biol.*, 686−694.
(49) Takamatsu, S., Hoshino, K., Matsumoto, K., Miyasaka, T., and Shimoyama, I. (2011) The photo charge of a bacterioRhodopsin

electrochemical cells measured by a charge amplifier. *IEICE Electron. Express 8*, 505−511.
(50) Imasheva, E. S., Balashov, S. P., Wang, J. M., and Lanyi, J. K. (2006) pH-Dependent transitions in xanthorhodopsin. *Photochem. Photobiol. 82*, 1406−1413.
(51) Hashimoto, K., Choi, A. R., Furutani, Y., Jung, K.-H., and Kandori, H. (2010) Low-Temperature FTIR Study of Gloeobacter Rhodopsin: Presence of Strongly Hydrogen-Bonded Water and Long-Range Structural Protein Perturbation upon Retinal Photoisomerization. *Biochemistry 49*, 3343−3350.
(52) Váró, G., and Lanyi, J. K. (1989) Photoreactions of bacteriorhodopsin at acid pH. *Biophys. J. 56*, 1143−1151.
(53) Balashov, S. P., Imasheva, E. S., Govindjee, R., and Ebrey, T. G. (1996) Titration of aspartate-85 in bacteriorhodopsin: what it says about chromophore isomerization and proton release. *Biophys. J. 70*, 473−481.
(54) Kelemen, L., Galajda, P., Szaraz, S., and Ormos, P. (1999) Chloride ion binding to bacteriorhodopsin at low pH: An infrared spectroscopic study. *Biophys. J. 76*, 1951−1958.
(55) Lenz, M. O., Huber, R., Schmidt, B., Gilch, P., Kalmbach, R., Engelhard, M., and Wachtveitl, J. (2006) First steps of retinal photoisomerization in proteorhodopsin. *Biophys. J. 91*, 255−262.
(56) Garavelli, M., Vreven, T., Celani, P., Bernardi, F., Robb, M. A., and Olivucci, M. (1998) Photoisomerization path for a realistic retinal chromophore model: The nonatetraeniminium cation. *J. Am. Chem. Soc. 120*, 1285−1288.
(57) Schapiro, I., Ryazantsev, M. N., Frutos, L. M., Ferre, N., Lindh, R., and Olivucci, M. (2011) The Ultrafast Photoisomerizations of Rhodopsin and Bathorhodopsin Are Modulated by Bond Length Alternation and HOOP Driven Electronic Effects. *J. Am. Chem. Soc. 133*, 3354−3364.
(58) Gonzalez-Luque, R., Garavelli, M., Bernardi, F., Merchan, M., Robb, M. A., and Olivucci, M. (2000) Computational evidence in favor of a two-state, two-mode model of the retinal chromophore photoisomerization. *Proc. Natl. Acad. Sci. U.S.A. 97*, 9379−9384.
(59) Schenkl, S., van Mourik, F., van der Zwan, G., Haacke, S., and Chergui, M. (2005) Probing the Ultrafast Charge Translocation of Photoexcited Retinal in Bacteriorhodopsin. *Science 309*, 917−920.
(60) Mathies, R., and Stryer, L. (1976) Retinal has a highly dipolar vertically excited singlet-state - implications for vision. *Proc. Natl. Acad. Sci. U.S.A. 73*, 2169−2173.
(61) Song, L., Elsayed, M. A., and Lanyi, J. K. (1993) Protein Catalysis of the Retinal Subpicosecond Photoisomerization in the Primary Process of Bacteriorhodopsin Photosynthesis. *Science 261*, 891−894.
(62) Cembran, A., Bernardi, F., Olivucci, M., and Garavelli, M. (2004) Counterion controlled photoisomerization of retinal chromophore models: a computational investigation. *J. Am. Chem. Soc. 126*, 16018−16037.
(63) Sineshchekov, O. A., and Spudich, J. L. (2004) Light-induced intramolecular charge movements in microbial rhodopsins in intact E. coli cells. *Photochem. Photobiol. Sci. 3*, 548−554.
(64) Koch, M. K., and Oesterhelt, D. (2005) MpcT is the transducer for membrane potential changes in Halobacterium salinarum. *Mol. Microbiol. 55*, 1681−1694.
(65) Hu, J., Griffin, R. G., and Herzfeld, J. (1994) Synergy in the spectral tuning of retinal pigments: complete accounting of the opsin shift in bacteriorhodopsin. *Proc. Natl. Acad. Sci. U.S.A. 91*, 8880−8884.
(66) Pfleger, N., Worner, A. C., Yang, J., Shastri, S., Hellmich, U. A., Aslimovska, L., Maier, M. S. M., and Glaubitz, C. (2009) Solid-state NMR and functional studies on proteorhodopsin. *Biochim. Biophys. Acta, Bioenerg. 1787*, 697−705.